



HAL
open science

Orientation dispersion estimated from multidimensional diffusion MRI: does it match simulated realistic microstructure?

Constance Bocquillon, Juan Luis Villarreal Haro, Jonathan Rafael Patino Lopez, Jean-Philippe Thiran, Isabelle Corouge, Emmanuel Caruyer

► To cite this version:

Constance Bocquillon, Juan Luis Villarreal Haro, Jonathan Rafael Patino Lopez, Jean-Philippe Thiran, Isabelle Corouge, et al.. Orientation dispersion estimated from multidimensional diffusion MRI: does it match simulated realistic microstructure?. ESMRMB 2024 - 40th Annual Meeting scientific European Society for Magnetic Resonance in Medecine and Biology, Oct 2024, Barcelone, Spain. pp.1-5, 2024. hal-04795839

HAL Id: hal-04795839

<https://hal.science/hal-04795839v1>

Submitted on 21 Nov 2024

HAL is a multi-disciplinary open access archive for the deposit and dissemination of scientific research documents, whether they are published or not. The documents may come from teaching and research institutions in France or abroad, or from public or private research centers.

L'archive ouverte pluridisciplinaire **HAL**, est destinée au dépôt et à la diffusion de documents scientifiques de niveau recherche, publiés ou non, émanant des établissements d'enseignement et de recherche français ou étrangers, des laboratoires publics ou privés.



Distributed under a Creative Commons Attribution 4.0 International License

Orientation dispersion estimated from multidimensional diffusion MRI: does it match simulated realistic microstructure?

Constance Bocquillon¹, Juan Luis Villarreal Haro², Jonathan Rafael Patino Lopez^{2,3}, Jean-Philippe Thiran^{2,3,4}, Isabelle Corouge¹, and Emmanuel Caruyer¹.

¹ University of Rennes, INRIA, CNRS, INSERM, IRISA UMR 6074, Empenn ERL U-1228, Rennes, France. ² Signal Processing Laboratory (LTS5), École Polytechnique Fédérale de Lausanne (EPFL), Lausanne, Switzerland. ³ Radiology Department, Centre Hospitalier Universitaire Vaudois (CHUV) and University of Lausanne (UNIL) (CHUV-UNIL), Lausanne, Switzerland. ⁴ CIBM Center for Biomedical Imaging, Lausanne, Switzerland.

Introduction:

In diffusion MRI, biophysical models promise to provide measures directly related to tissue microstructure^{1,2,3}. This is made possible at the cost of modeling assumptions, which can be invalidated in pathological situations⁴. In contrast, the diffusion tensor distribution (DTD) framework⁵ characterizes the distribution of Gaussian diffusion compartments inside a voxel, from which estimates of the microscopic anisotropy (μ FA) or the orientation parameter (OP) can be computed. The objective of this work is to help with the interpretation of such parameters by comparing them with microstructure features in simulated substrates of white matter.

Methods: Substrate generation. We generated a collection of 11 numerical substrates using CACTUS⁶. Briefly, we employed a two steps procedure: the first step initializes the substrate with a single fiber population with a given dispersion angle and fixed radii distribution. The second step minimizes fiber overlap and extreme curvature. We did not use the third step to increase packing⁶ as it was not a priority for this experiment and increased the computational cost.

The collection has an intracellular volume fraction at 0.72 and a gamma distributed radius ($\kappa = 1$, mean radius = $2.5\mu\text{m}$). The only parameter that varies across the substrates is the dispersion which ranges from 0° to 25° in steps of 2.5° . The substrates are cubes with a side length of $200\mu\text{m}$.

Orientation parameter. We wanted to link the dispersion of our substrate with the orientation parameter (OP) described in QTI⁵. This parameter, which ranges from 0 to 1, geometrically describes the orientation of the diffusion tensors distribution with $\text{OP}=0$ for isotropically oriented tensors and $\text{OP}=1$ for perfectly aligned tensors.

To serve as a reference, we estimated a ground truth, geometric OP_{gt} , from the substrates. We decomposed the fiber centerlines into fixed-length segments, which we assimilated to rank-1 tensors, from which we computed OP_{gt} ⁵. Note that the segment length impacts this estimation of OP_{gt} , with larger segments smoothing out micro-undulations, resulting in larger OP_{gt} . To be comparable to the orientation dispersion estimated from the DTD, we advocate choosing a segment length in the same order as the characteristic diffusion length, which is $\sqrt{2D\tau}$, where τ is the effective diffusion time; we evaluated τ in the range 60-80ms, which corresponds to a characteristic diffusion length of 15-18 μm .

Signal simulation and DTD estimation. The signal was generated for an acquisition scheme optimized for the reconstruction of several DTD parameters⁷. This scheme includes linear, spherical and planar tensor encoding (LTE, STE and PTE, respectively; see Fig.1). We used the numerically optimized waveforms⁸ to generate a gradient trajectory for a spherical b-tensor; this trajectory was then modified by applying proper scaling and rotation⁵ to generate 120 waveforms corresponding to the acquisition scheme.

The intra-cellular and extra-cellular contributions to the signal were simulated separately through Monte-Carlo simulation⁹ for each substrate. We generated 10^6 particles diffusing during 101ms with 1000 timesteps, with a diffusivity of $2\mu\text{m}^2/\text{ms}$.

The estimation of the DTD parameters and the OP from the simulated signal was done using the QTI implementation of Dipy¹⁰.

Results: Figure 2 shows 2 substrates corresponding to angular dispersion of 5° and 25° . The link between these angular dispersions and OP_{gt} is illustrated in Figure 3 for a range of segment lengths (from 1 to $100\mu\text{m}$). For a given substrate, OP_{gt} increases with the segment length.

Figure 4 plots the OP estimated from the DTD with respect to geometric OP_{gt} , for the same range of

segment lengths. For both the intracellular and extracellular signals, the OP estimated from the DTD is strongly correlated to OP_{gt} . The bottom figure suggests that when we have dispersion in the substrate, we can no longer model the extracellular part of the signal as a single gaussian compartment, which contradicts the assumptions made in most biophysical models of white matter^{1,2,3}.

Discussion and conclusions: In realistic white matter substrates, there is a clear link between the estimated OP from the diffusion signal and the dispersion of fibers. The extra-axonal diffusion is complex and cannot be represented by a single diffusion tensor.

Future work includes extending the range of orientation dispersion within the substrate and testing the effect of the acquisition scheme. It would also be interesting to study the link between the microscopic anisotropy and geometric properties of the substrates (e.g. axonal radius or density), and to assess the influence of these parameters on the estimation of OP.

Last, the substrates we generated are composed exclusively of white matter fibers. The presence of other cell structures (glial cells, soma, etc.) could also influence the estimation of mathematical parameters and needs to be taken into consideration.

References:

1. Zhang, H., Schneider, T., Wheeler-Kingshott, C. A., & Alexander, D. C. (2012). NODDI: practical in vivo neurite orientation dispersion and density imaging of the human brain. *Neuroimage*, 61(4), 1000-1016.
2. Assaf, Y., & Basser, P. J. (2005). Composite hindered and restricted model of diffusion (CHARMED) MR imaging of the human brain. *Neuroimage*, 27(1), 48-58.
3. Assaf, Y., Blumenfeld-Katzir, T., Yovel, Y., & Basser, P. J. (2008). AxCaliber: a method for measuring axon diameter distribution from diffusion MRI. *Magnetic Resonance in Medicine: An Official Journal of the International Society for Magnetic Resonance in Medicine*, 59(6), 1347-1354.
4. Lampinen B, Szczepankiewicz F, Mårtensson J, van Westen D, Sundgren PC, Nilsson M. Neurite density imaging versus imaging of microscopic anisotropy in diffusion MRI: A model comparison using spherical tensor encoding. *Neuroimage*. 2017;147:517-531.
5. Westin CF, Knutsson H, Pasternak O, et al. Q-space trajectory imaging for multidimensional diffusion MRI of the human brain. *Neuroimage*. 2016;135:345-362.
6. Villarreal-Haro JL, Gardier R, Canales-Rodríguez EJ, et al. CACTUS: a computational framework for generating realistic white matter microstructure substrates. *Front Neuroinform*. 2023;17:1208073.
7. Morez J, Szczepankiewicz F, den Dekker AJ, Vanhevel F, Sijbers J, Jeurissen B. Optimal experimental design and estimation for q-space trajectory imaging. *Hum Brain Mapp*. 2023;44(4):1793-1809.
8. Sjölund J, Szczepankiewicz F, Nilsson M, Topgaard D, Westin CF, Knutsson H. Constrained optimization of gradient waveforms for generalized diffusion encoding. *J Magn Reson*. 2015;261:157-168.
9. Rafael-Patino J, Romascano D, Ramirez-Manzanares A, Canales-Rodríguez EJ, Girard G, Thiran JP. Robust Monte-Carlo Simulations in Diffusion-MRI: Effect of the Substrate Complexity and Parameter Choice on the Reproducibility of Results. *Front Neuroinform*. 2020;14:8.
10. Garyfallidis E, Brett M, Amirbekian B, et al. Dipy, a library for the analysis of diffusion MRI data. *Front Neuroinform*. 2014;8:8.

Summary:

We compared the diffusion tensor distribution parameters to microstructure features in realistic, simulated substrates in diffusion MRI. The orientation parameter is related to the actual angular dispersion of white matter fibers; extra-axonal signal reveals complex, non-Gaussian diffusion.

Figures:

$b(\text{ms}/\mu\text{m}^2)$	PTE	STE	LTE
0.1	7	-	9
0.8	9	-	50
2	-	30	15

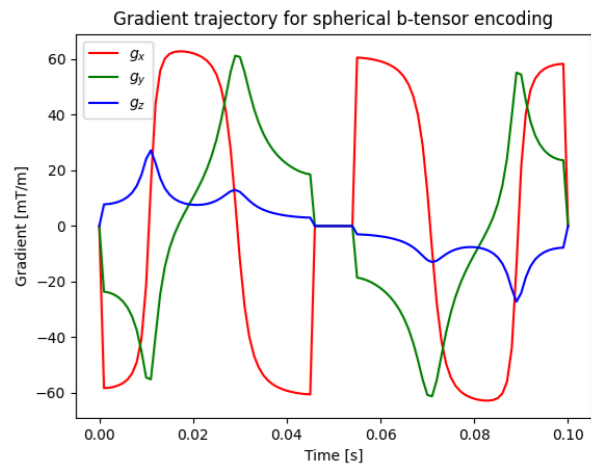


Figure 1: (left) Repartition of the 120 b-tensor encoded acquisitions corresponding to the Q_3 scheme⁷ used for the simulations; (right) template gradient trajectory to implement the spherical tensor encoding (STE) b-tensors.



Figure 2: Realistic white matter substrates generated with CACTUS⁶ with angular dispersion of 5° (left) and 25° (right).

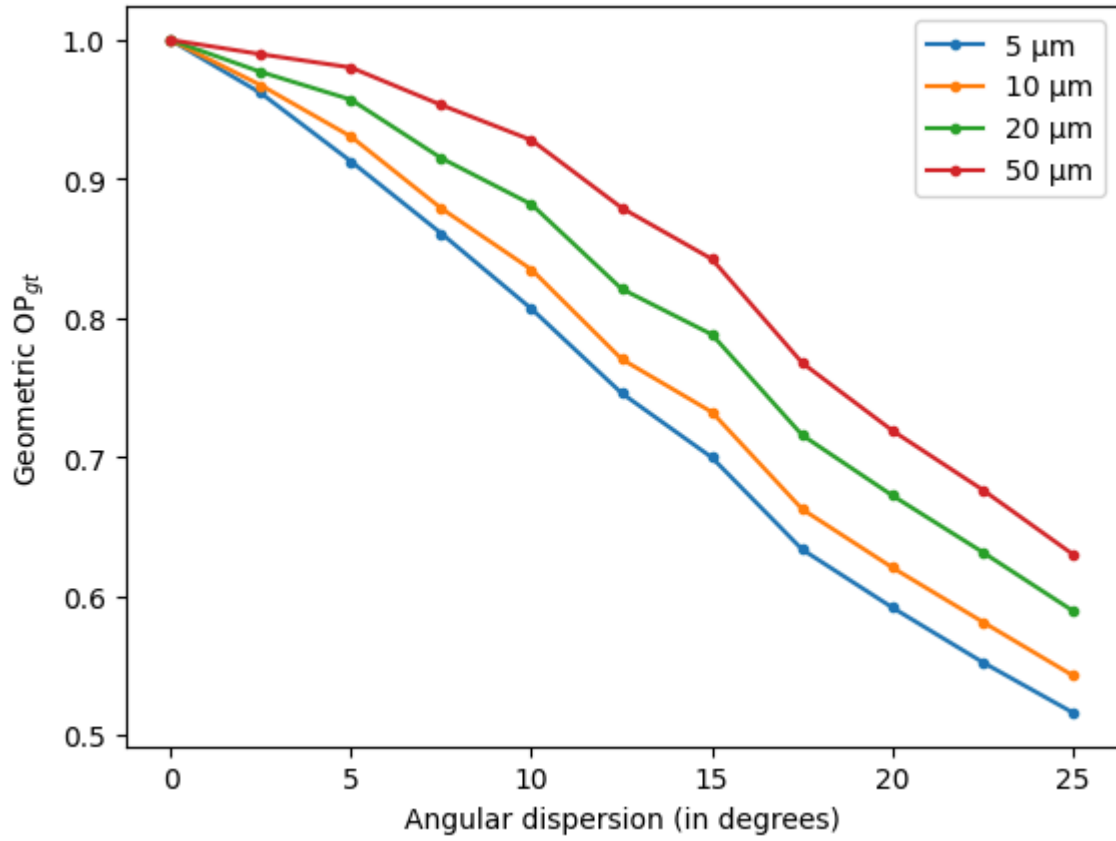


Figure 3: Geometric OP_{gt} computed for several lengths of segments as a function of the target dispersion for our collection of substrates.

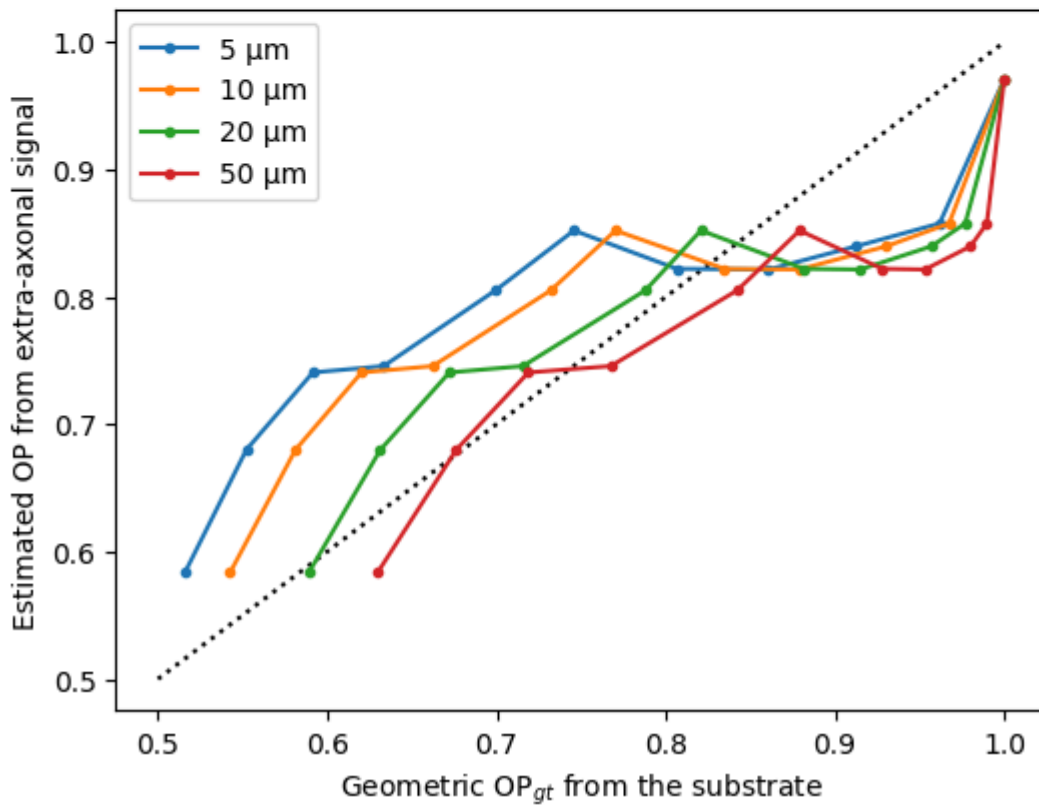
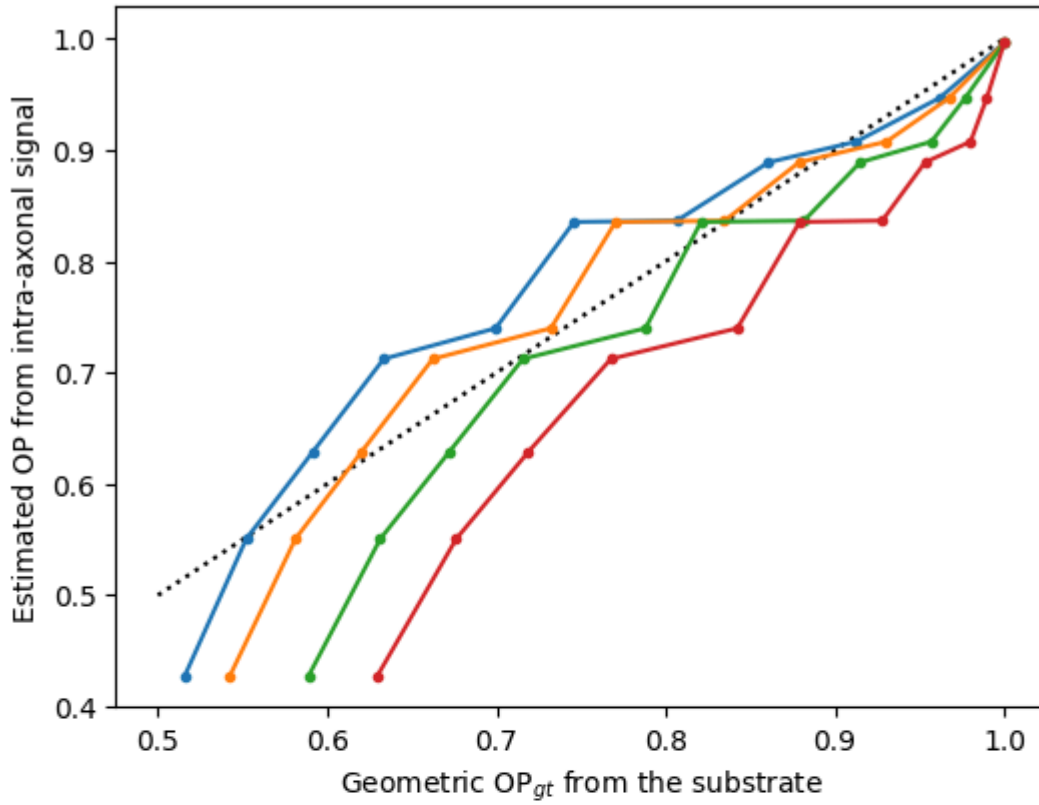


Figure 4: Estimated OP from the signal for our collection of substrates as a function of geometric OP_{gt} computed from the substrate for several lengths of segments for the intra-cellular signal (top) and extra-cellular signal (bottom).